Journal of Materials Chemistry

Cite this: J. Mater. Chem., 2012, 22, 23272

www.rsc.org/materials

PAPER

Self-powered and fast-speed photodetectors based on CdS:Ga nanoribbon/Au Schottky diodes

Di Wu,[a] Yang Jiang,*[a] Yugang Zhang,[a] Yongqiang Yu,[a] Zhifeng Zhu,[a] Xinzheng Lan,[a] Fangze Li,[b] Chunyan Wu,[b] Li Wang[b] and Linbao Luo*[b]

Received 24th July 2012, Accepted 13th September 2012
DOI: 10.1039/c2jm34869a

Self-powered photodetectors based on CdS:Ga nanoribbons (NR)/Au Schottky barrier diodes (SBDs) were fabricated. The as-fabricated SBDs exhibit an excellent rectification characteristic with a rectification ratio up to 10^6 within ± 1 V in the dark and a distinctive photovoltaic (PV) behavior under light illumination. Photoconductive analysis reveals that the SBDs were highly sensitive to light illumination with very good stability, reproducibility and fast response speeds at zero bias voltage. The corresponding rise/fall times of 95/290 μs represent the best values obtained for CdS based nano-photodetectors. It is expected that such self-powered high performance SBD photodetectors will have great potential applications in optoelectronic devices in the future.

I. Introduction

Photodetectors (PDs) that can convert light into electrical signal are crucial for wide applications in many fields, such as imaging techniques, light-wave communications, memory storage and optoelectronic circuits.[1–6] High-performance PDs with fast speeds and low-power consumption are highly desired for applications of optoelectronic integration. Recent progress in PDs demonstrates that the device structure of the PDs plays important roles in determining the detection ability. For instance, *Ohmic* contact photodetectors (OPDs) normally exhibit unparalleled performance in terms of high responsivity (R) and high photoconductive gain (G), whereas Schottky junction photodetectors (SPDs) and heterojunction photodetectors (HPDs) in contrast have advantages in sensitivity and fast response speeds.[7–9] In addition, photovoltaic (PV) behavior usually can be observed in such Schottky and heterojunction based devices, which can provide energy for themselves in applications of PDs.[8,10] This feature renders it possible to detect light irradiation without an exterior power supply.

Due to the unique properties in electrical transport and light absorption, one-dimensional (1D) inorganic nanostructure semiconductors such as nanowires (NWs), nanoribbons (NRs) and nanotubes (NTs) have attracted extensive attention in the past few decades.[11–15] In comparison with PDs based on traditional thin-film and bulk materials, PDs made from 1D semiconductor nanostructures usually have the advantage of higher responsivity and photoconductivity gain because of their high crystallinity and high surface-to-volume ratio.[16–18] Moreover, the reduced dimension of the effective conductive channel can shorten the carrier transit time, leading to a faster response speed.[9] Undoubtedly, 1D semiconductor nanostructures are promising candidates for high-performance PD applications. CdS is an important II–VI group semiconductor material and has been widely used in optoelectronic devices such as PDs, PV devices and so on.[8,19,20] To date, while great progress has been made in fabricating visible light photodetectors with high responsivity and high response speed, relatively little work has been focused on low-power, or even self-powered PDs, which will hold great promise in future nano-optoelectronic devices.[21,22]

In this paper, we present an investigation of self-powered PDs based on CdS:Ga NR/Au Schottky barrier diodes (SBDs). The SBD exhibits an excellent rectification characteristic in the dark and shows a clear PV behavior under light illumination. The photoresponse of the CdS:Ga NR/Au SPDs was studied at zero bias, which shows the excellent repeatability and stability of the SPDs with a fast response speed in a wide range of switching frequencies. These results suggest that the self-powered CdS:Ga NR/Au SPD may have important applications in future nano-optoelectronics integrated circuits.

II. Experimental

Undoped CdS nanomaterials are highly insulative semiconductors with a very low conduction current of $\sim 10^{-14}$ A, which cannot function as elementary components for nano-photodetectors.[17,20] Hence, the Ga doped CdS NRs employed in this work were synthesized by using CdS powder (99.99%, Aldrich) and Ga–Ga_2O_3 powder as the source material and the n-type dopant, respectively, *via* a co-thermal evaporation method in a horizontal tube furnace.[8,20] Although the melting point of

[a]*School of Materials Science and Engineering, Hefei University of Technology, Hefei, Anhui 230009, P. R. China. E-mail: apjiang@hfut.edu.cn*
[b]*School of Electronic Science and Applied Physics, Hefei University of Technology, Hefei, Anhui 230009, P. R. China. E-mail: luolb@hfut.edu.cn*

elementary gallium is very low (~30 °C), its boiling point is too high (~2400 °C) to be evaporated. Hence, a mixture of Ga and Ga_2O_3 powders was used as the dopant source material in this work. Ga vapor could be generated through the following reactions at a relatively low temperature (>600 °C):

$$4Ga(l) + Ga_2O_3(s) \rightarrow 3Ga_2O(g) \quad (1)$$

$$Ga_2O(g) + H_2(g) \rightarrow 2Ga(g) + H_2O(g) \quad (2)$$

In detail, about 0.5 g CdS, Ga and Ga_2O_3 mixed powder was firstly loaded onto an alumina boat and transferred to the center region of the tube furnace. In this work, three samples with various levels of Ga doping were synthesized, corresponding to the increased Ga and Ga_2O_3 mixture to CdS mass ratio of 2%, 4% and 8%, respectively. Undoped CdS NRs were also synthesized under the same conditions for comparison. Si substrates coated with 10 nm gold catalyst were then placed at the downstream position about 10 cm away from the evaporation source. Before heating, the system was evacuated to a base pressure of 10^{-5} Torr, and back filled with an Ar and H_2 (5%) gas mixture at a constant flow rate of 60 sccm to a stable pressure of 150 Torr. Afterwards, the mixed powder was heated up to 880 °C and maintained at that temperature for 2 h. A layer of yellow wool-like product could be observed on the Si substrates surface after growth.

To construct the Schottky junction devices, the as-synthesized CdS:Ga NRs were dispersed in parallel on the SiO_2 (300 nm)/p^+-Si substrate by the contact print technique,[23] and then photolithography and electron beam evaporation were used to define indium (In, 100 nm) *Ohmic* contact electrodes on the NRs. Then the Au (20 nm) Schottky electrodes on the other side were defined by additional photolithography and electron beam evaporation. Fig. 3a shows a SEM image of an as-fabricated CdS:Ga NR/Au Schottky junction device. Electrical measurements were conducted at room temperature by using a semiconductor characterization system (Keithley 4200-SCS). The optoelectronic characteristics of the SBDs were analyzed by using a system that combines a monochromatic light source, an oscilloscope (Tektronix, TDS2012B) and an optical chopper (SRS, SR540), as shown in Fig. 6a.[7,8]

III. Results and discussion

Fig. 1a shows a typical FESEM image of the as-synthesized CdS:Ga NRs. It is seen that the NRs are clear and smooth with a uniform geometry, a width in the range of 1–5 μm, thickness of 50–200 nm and length of several tens of micrometers. The high-resolution transmission electron microscopy (HRTEM) image and the corresponding selected-area electron diffraction (SEAD) pattern also reveal that the NRs have a single-crystal wurtzite structure with a growth orientation of [001] as shown in Fig. 1b. In the XRD patterns (Fig. 1c), all the diffraction peaks can be assigned to wurtzite CdS (JCPDS 41-1049) and no impurity phases are detected, suggesting a high phase purity of the product. X-ray photoelectron spectroscopy (XPS) measurements were performed to further detect the compositions of the CdS:Ga NWs (8% Ga source doping), as shown in Fig. 1d. In addition to the Cd and S peaks, a peak at ~1118 eV that corresponds to the

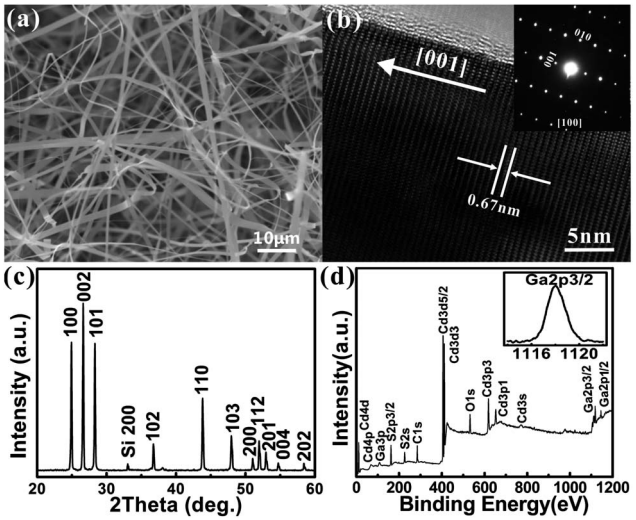

Fig. 1 (a) FESEM image, (b) HRTEM image, (c) XRD pattern and (d) XPS spectrum of the as-synthesized CdS:Ga NRs. The insets in (b) and (d) show the corresponding SAED pattern and the enlarged Ga peaks, respectively.

Ga2p3/2 core level appeared, revealing the successful incorporation of Ga in the CdS NRs with an estimated Ga content of ~2.1 at%, implying that efficient Ga doping is achieved in the CdS:Ga NRs.

The influence of Ga doping on the transport properties of the CdS NRs was assessed by the electrical measurements on an individual NR, as shown in Fig. 2. From the typical *I–V* curves of the samples, it is found that the undoped CdS NR exhibits an extremely low conduction current (~10^{-14} A). Its conductivity is estimated to be as low as 10^{-9} S cm^{-1}. In contrast, a substantial enhancement in the conductivity is observed for the CdS:Ga NRs. The conductivities increase dramatically to 2.65 × 10^{-2} S cm^{-1}, 1.76 × 10^{-1} S cm^{-1} and 1.1 S cm^{-1} for the 2%, 4% and 8% Ga source doped samples, respectively. To gain statistical significance, the conductivities of 30 NRs for each sample were measured and the corresponding conductivity histogram is depicted in Fig. 2b. Significantly, the conductivity of the CdS NRs could be tuned over a wide range of about ten orders of magnitude from 10^{-9} S cm^{-1} (undoped CdS) to 10 S cm^{-1} for the 8% Ga source doped sample. The remarkable increase in the conductivity is a result of the Ga doping in the CdS NRs, demonstrating that Ga could be a very efficient

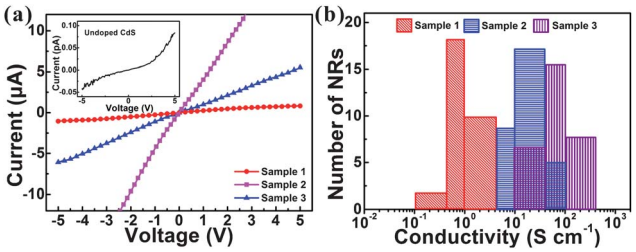

Fig. 2 (a) Typical *I–V* curves of the CdS NRs with varied doping levels in the dark. The inset shows the *I–V* curve of an undoped CdS NR for comparison. (b) A conductivity histogram for the three doped samples.

donor dopant to tune the electrical transport properties of the CdS NRs.

Fig. 3b depicts typical *I–V* curves of the CdS:Ga NR/Au SBDs measured in the dark for 2%, 4% and 8% Ga source doped samples. The SBDs show excellent rectification characteristics with a rectification ratio up to 10^6 within ±1 V. From the rectification curves, low turn-on voltages of ~0.5 V can be deduced at the forward bias direction. For an ideal diode, the rectification characteristics can be described by the following equations:

$$I_{DS} = I_0\left(e^{V_{DS}/nK_BT} - 1\right) \quad (3)$$

$$I_0 = AA^*T^2\exp\left(-\frac{q\Phi_{Bn}}{K_BT}\right) \quad (4)$$

where I_0 is the reverse saturation current, A the Schottky contact area, K_B the Boltzmann's constant, T the Kelvin temperature, A^* the Richardson's constant (~23 A $K^{-2}cm^{-2}$ for CdS) and Φ_{Bn} is the barrier height. By fitting the rectification curve (Fig. 3b) following the equation above, the ideality factor n and Φ_{Bn} are determined to be 1.3–1.4 and 0.74–0.76 eV, respectively. The ideality factor is close to the value of an ideal Schottky junction, and Φ_{Bn} is quite close to those reported for bulk single-crystal CdS/Au Schottky junctions.[24] These results also confirm that high-quality Schottky diodes were obtained.

The *I–V* curves of the CdS:Ga NR/Au SBDs under white light illumination with intensity of 7.4 mW cm^{-2} are depicted in Fig. 3c, from which, a pronounced PV effect could be observed. The open-circuit photovoltage (V_{OC}) and a short circuit current (I_{SC}) are deduced to be 0.16 V–0.18 V and 0.73 nA–1.05 nA, respectively, leading to a maximum fill factor (FF) of 29.9% for the 8% Ga source doped sample. The principle of such Schottky junction PV devices can be understood from the energy band diagrams shown in Fig. 4. Like the traditional Schottky junction

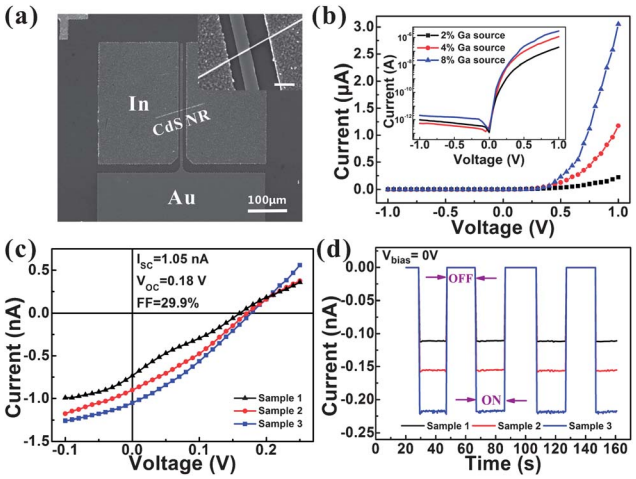

Fig. 3 (a) SEM image of CdS NR/Au Schottky diode. Inset shows an enlarged SEM image, the scale bar is 10 μm. (b) Rectification characteristic and (c) photovoltaic characteristic of the CdS:Ga NR/Au SBD for 2%, 4% and 8% Ga source doped samples measured in the dark and under light illumination with intensity of 7.4 mW cm^{-2}. (d) Time response of CdS:Ga NR/Au SPDs at zero bias under light illumination of 510 nm with intensity of 0.27 mW cm^{-2}.

based solar cell, the gold thin film (20 nm), that is somewhat transparent to visible light, allows the effective absorption of photons with energy greater than E_g by semiconductor nanostructures. As a result, the electrons were driven into the CdS, and the holes were driven into the Au surface, as soon as the photogenerated electron–hole pairs were readily separated by the built-in field within the depletion region. The continuous accumulation of these carriers at both sides of the depletion region forms the photo-voltage with a direction pointing from metal to semiconductor. Once the Schottky junction is short-circuited (Fig. 4b), the photo-generated carriers can transit through the external circuit, giving rise to a short circuit current.

Remarkably, this CdS:Ga NR/Au SBDs can function as a high-performance self-powered visible light photodetector. Fig. 3d shows the reversible switching between high and low conductance without exterior power supply, when 510 nm light illumination with intensity of 0.27 mW cm^{-2} was turned on and off. The I_{on}/I_{off} ratio is ~10^3. What is more, the responses of all three SBDs was very fast and highly stable and reproducible. Responsivity and photoconductivity gain for a PD can be estimated according to the following relation:

$$R = \frac{I_P}{P_{opt}} = \eta\left(\frac{q\lambda}{hc}\right)G \quad (5)$$

where I_p is the photocurrent, P_{opt} the incident light power, η the quantum efficiency, h is Planck's constant, λ the light wavelength and c the light speed. Based on this equation, R and G were estimated to be ~4 A W^{-1} and 10 for 2% Ga source doping sample, ~6 A W^{-1} and 15 for 4% Ga source doping sample, ~8 A W^{-1} and 20 for 8% Ga source doping sample, respectively, at 0 V for the CdS:Ga NRs based SPDs. The greater-than-unity gain may be attributed to the high-quality of the doped CdS NRs and the prolonged carrier lifetime. Due to oxygen adsorption, both at the surface of the CdS NR and the Schottky contact from the ambient environment, the electrons and holes were separated by the strong local electrical field existing at the Au/NR interface, as a result, the electron–hole recombination was largely restricted.[14,25]

CdS is a promising material for photodetectors due to its primary band-gap of 2.4 eV at room temperature. Fig. 5 depicts the spectral response of the CdS:Ga NR and CdS SPD when the devices were exposed to monochromatic light at a constant intensity of 1.0 mW cm^{-2}. Notably, both CdS NR and SPD show a pronounced photoresponse to the short wavelength light. From the curves, it is seen that sensitivity is highest around 510 nm and shows a steep decline in the long wavelength direction. For CdS NR, the cut-off wavelength of 510 nm is consistent with CdS

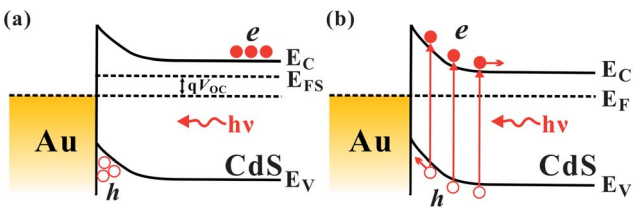

Fig. 4 The energy band diagrams of (a) an open-circuited and (b) a short-circuited CdS:Ga NR/Au Schottky junction device under light illumination.

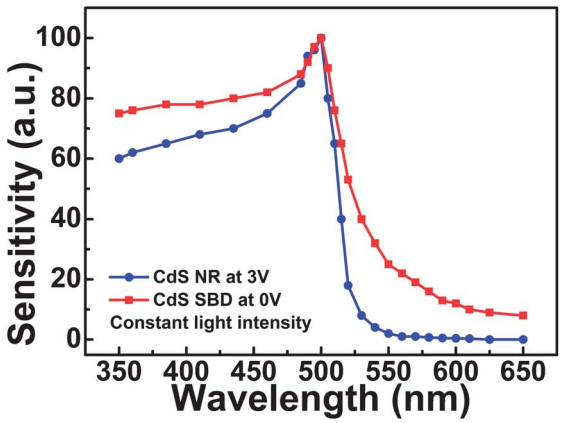

Fig. 5 Spectral response of the CdS:Ga NR and CdS SBD when the devices were exposed to monochromatic light at a constant intensity of 1.0 mW cm^{-2}.

band-gap, indicating that the electron–hole pairs excited by light with energy larger than the band-gap of CdS should account for the photocurrent. But for the CdS/Au SPD, the spectrum is extended to longer wavelengths and more sensitivity than CdS NR in the long wavelength direction. This may be due to the internal electrons of CdS that will transfer from the defect level to the conduction band after absorbing photons and photons with energy less than the band-gap of CdS excited metallic electrons through the Schottky barrier and are then collected by the conduction band of CdS.[26]

To explore the capability to follow a fast-varying optical signal, which is particularly important in lightwave communication and optical-switch applications,[7–9] the photoresponse of the CdS:Ga NR/Au SPD (8% Ga source doped sample) was further studied under zero bias by modulating the incident light with a mechanical chopper (Fig. 6a). Considering the high frequency of the illumination switching, an oscilloscope was used to monitor the variation of the photocurrent with time. Fig. 6b–d show the reversible switching of the SPD between low and high conduction states when the light was turned on and off regularly (the data was normalized according to the highest photocurrent). Significantly, the SPD could operate with excellent stability and reproducibility in a wide frequency range from 1 to 500 Hz under light illumination of 510 nm with intensity of 0.27 mW cm^{-2}. Moreover, as shown in Fig. 6e, the relative balance $(I_{max} - I_{min})/I_{max}$ of the photocurrent only decreases by less than 5% at a high frequency of 500 Hz, which is much less than the values of OPD (~30% at 500 Hz)[12] and HPD (~5% at 400 Hz),[8] implying that the CdS:Ga SPD can even monitor an optical signal with much higher frequency.[11] In the time domain, the speed of a PD is often characterized by the rise time (τ_r) and the fall time (τ_f) of its response to an impulse signal or to a pulse signal.[27] Further analysis to the SPD reveals a small τ_r of 95 μs, as well as a small τ_f of 290 μs (Fig. 6f). These response times are much quicker than the 746/794 μs of CdS OPD[12] and 300/740 μs of CdS HPD,[8] representing the best value obtained for the CdS based nano-PDs.

The fast response speed is believed to be associated with the high-quality Schottky junction between the CdS:Ga NR and the Au electrode. When the Schottky junction was irradiated with visible light, this light will be absorbed. Due to few interface

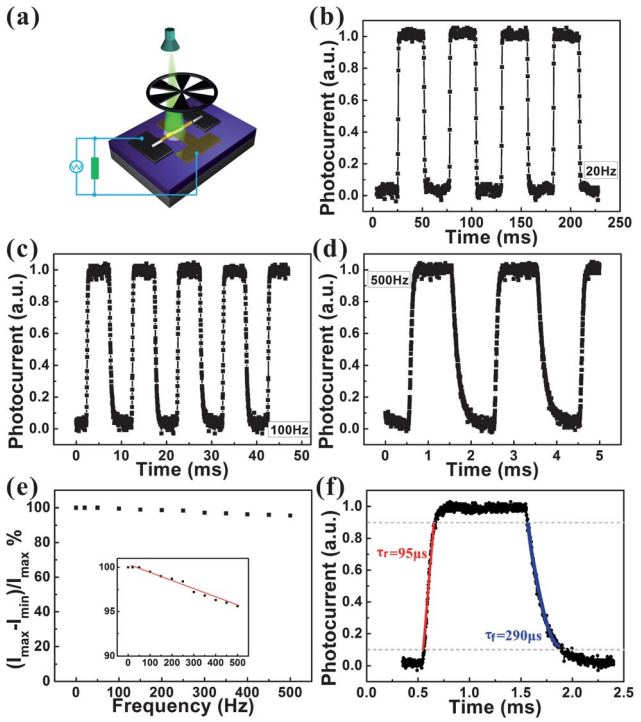

Fig. 6 (a) Schematic illustration of the measurement configuration for photoresponse detection. Photoresponse characteristics of the CdS:Ga NR/Au SPD to pulsed light irradiation at frequency of (b) 20 Hz, (c) 100 Hz and (d) 500 Hz. (e) The relative balance $[(I_{max} - I_{min})/I_{max}]$ *versus* switching frequency. Inset shows the enlarged image. (f) Rising and falling edges for estimating the rise and fall times.

defects, the resultant photo-generated electron–hole pairs could be quickly separated and then transferred to the electrodes by the built-in electric field, leading to the fast response speed. Reasonably, as these two values are highly dependent on light intensity, the τ_r and τ_f could be further reduced by increasing the light intensity.[11] These results suggest that the meritorious characteristics of the high-quality CdS:Ga NR/Au SBD photodetector, such as high-speed and no energy consumption, will afford new opportunities for future nano-optoelectronic device applications.

IV. Conclusions

In summary, self-powered PDs based on CdS:Ga NR/Au SBDs have been demonstrated. The SBDs exhibit an excellent rectification characteristic with a rectification ratio of up to 10^6 within ±1 V in the dark and a pronounced PV effect under light illumination. Further photoresponse analysis showed that such CdS:Ga NR/Au SPDs can work under zero bias, with high photosensitivity and the greater-than-unity gain. Moreover, the fastest response speed was achieved for CdS based nano-PDs. It is expected that these self-powered CdS:Ga NR/Au SPDs with fast-speeds will have potential applications in nano-optoelectronic integrated circuits.

Acknowledgements

This work was supported by financial support from the National High Technology Research and the Development Program of

China (no. 2007AA03Z301), the National Natural Science Foundation of China (nos. 20771032, 61076040, 20901021, 21101051 and 61106010) and the National Basic Research Program of China (no. 2007CB9-36001).

Notes and references

1 J. Wang, M. S. Gudiksen, X. Duan, Y. Cui and C. M. Lieber, *Science*, 2001, **293**, 1455.
2 H. Kind, H. Q. Yan, B. Messer, M. Law and P. D. Yang, *Adv. Mater.*, 2002, **14**, 158.
3 Q. Bao and K. P. Loh, *ACS Nano*, 2012, **6**, 3677.
4 C. Li, Y. Bando, M. Y. Liao, Y. Koide and D. Golberg, *Appl. Phys. Lett.*, 2010, **97**, 161102.
5 P. C. Wu, Y. Dai, Y. Ye, Y. Yin and L. Dai, *J. Mater. Chem.*, 2011, **21**, 2563.
6 T. Y. Zhai, L. Li, X. Wang, X. S. Fang, Y. Bando and D. Golberg, *Adv. Funct. Mater.*, 2010, **20**, 4233.
7 D. Wu, Y. Jiang, Y. G. Zhang, J. W. Li, Y. Q. Yu, Y. P. Zhang, Z. F. Zhu, L. Wang, C. Y. Wu, L. B. Luo and J. S. Jie, *J. Mater. Chem.*, 2012, **22**, 6206.
8 D. Wu, Y. Jiang, S. Y. Li, F. Z. Li, J. W. Li, X. Z. Lan, Y. G. Zhang, C. Y. Wu, L. B. Luo and J. S. Jie, *Nanotechnology*, 2011, **22**, 405201.
9 P. C. Wu, Y. Dai, T. Sun, Y. Ye, H. Meng, X. L. Fang, B. Yu and L. Dai, *ACS Appl. Mater. Interfaces*, 2011, **3**, 1859.
10 Y. Ye, L. Dai, P. C. Wu, C. Liu, T. Sun, R. M. Ma and G. G. Qin, *Nanotechnology*, 2009, **20**, 375202.
11 Y. Jiang, W. J. Zhang, J. S. Jie, X. M. Meng, X. Fan and S. T. Lee, *Adv. Funct. Mater.*, 2007, **17**, 1795.
12 J. S. Jie, W. J. Zhang, Y. Jiang, X. M. Meng, Y. Q. Li and S. T. Lee, *Nano Lett.*, 2006, **6**, 1887.
13 L. B. Luo, X. B. Yang, F. X. Liang, J. S. Jie, Q. Li, Z. F. Zhu, C. Y. Wu, Y. Q. Yu and L. Wang, *CrystEngComm*, 2012, **14**, 1942.
14 T. Y. Wei, C. T. Huang, B. J. Hansen, Y. F. Lin, L. J. Chen, S. Y. Lu and Z. L. Wang, *Appl. Phys. Lett.*, 2010, **96**, 013508.
15 T. Y. Zhai, L. Li, Y. Ma, M. Y. Liao, X. Wang, X. S. Fang, J. N. Yao, Y. Bando and D. Golberg, *Chem. Soc. Rev.*, 2011, **40**, 2986.
16 Y. Q. Yu, J. S. Jie, P. Jiang, L. Wang, C. Y. Wu, Q. Peng, X. W. Zhang, Z. Wang, C. Xie, D. Wu and Y. Jiang, *J. Mater. Chem.*, 2011, **21**, 12632.
17 C. Y. Wu, J. S. Jie, L. Wang, Y. Q. Yu, Q. Peng, X. W. Zhang, J. J. Cai, H. E. Guo, D. Wu and Y. Jiang, *Nanotechnology*, 2010, **21**, 505203.
18 R. S. Chen, T. H. Yang, H. Y. Chen, L. C. Chen, K. H. Chen, Y. J. Yang, C. H. Su and C. R. Lin, *Appl. Phys. Lett.*, 2009, **95**, 162112.
19 R. M. Ma, L. Dai and G. G. Qin, *Nano Lett.*, 2007, **7**, 868.
20 J. J. Cai, J. S. Jie, P. Jiang, D. Wu, C. Xie, C. Y. Wu, Z. Wang, Y. Q. Yu, L. Wang, X. W. Zhang, Q. Peng and Y. Jiang, *Phys. Chem. Chem. Phys.*, 2011, **13**, 14663.
21 S. Xu, Y. Qin, C. Xu, Y. Wei, R. Yang and Z. L. Wang, *Nat. Nanotechnol.*, 2010, **5**, 366.
22 Y. Yang, W. Guo, J. J. Qi, J. Zhao and Y. Zhang, *Appl. Phys. Lett.*, 2010, **97**, 223113.
23 W. S. Wong, S. Raychaudhuri, R. Lujan, S. Sambandan and R. A. Street, *Nano Lett.*, 2011, **11**, 2214.
24 S. Oktik, G. Russell and J. Woods, *Semicond. Sci. Technol.*, 1987, **2**, 661.
25 W. F. Jin, Y. Ye, L. Gan, B. Yu, P. C. Wu, Y. Dai, H. Meng, X. F. Guo and L. Dai, *J. Mater. Chem.*, 2012, **22**, 2863.
26 J. Y. Duboz, N. Grandjean, F. Omnes, M. Mosca and J. L. Reverchon, *Appl. Phys. Lett.*, 2005, **86**, 063511.
27 N. Joshi and B. Thompson, *Photoconductivity*, Dekker, New York, 1990.

